Journal of Applied Polymer Science

Polyurethane/poly(ethylene-*co*-ethyl acrylate) and functional carbon black-based hybrids: Physical properties and shape memory behavior

Ayesha Kausar,[1] Muhammad Siddiq[2]

[1]Nanosciences Division, National Centre for Physics, Quaid-i-Azam University Campus, Islamabad 44000, Pakistan

[2]Department of Chemistry, Quaid-i-Azam University, Islamabad 45320, Pakistan

Correspondence to: A. Kausar (E-mail: asheesgreat@yahoo.com)

ABSTRACT: A polyurethane (PU) was developed from poly(dimethylamine-*co*-epichlorohydrin-*co*-ethylenediamine) (PDMAE) and polyethylene glycol (PEG) as soft segment and 2,4-toluene diisocyanate (TDI) incorporating as hard segment. Later PU was blended with poly(ethylene-*co*-ethyl acrylate) (PEEA). Poly(vinyl alcohol)-functionalized carbon black (CB-PVA) nanoparticles was used as filler. The structure, morphology, mechanical, crystallization, and shape memory behavior (heat and voltage) were investigated methodically. Due to physical interaction of the blend components, unique self-assembled network morphology was observed. The interpenetrating network was responsible for 83% rise in tensile modulus and 46% increase in Young's modulus of PU/PEEA/CB-PVA 1 hybrid compared with neat PU/PEEA bend. Electrical conductivity was increased to 0.2 Scm^{-1} with 1 wt % CB-PVA nanofiller. The original shape of sample was almost 94% recovered using heat induced shape memory effect while 97% recovery was observed in an electric field of 40 V. Electroactive shape memory results were found better than heat stimulation effect. © 2016 Wiley Periodicals, Inc. J. Appl. Polym. Sci. **2016**, *133*, 43481.

KEYWORDS: blends; differential scanning calorimetry (DSC); morphology; polyurethanes; synthesis and processing

Received 7 December 2015; accepted 28 January 2016

DOI: 10.1002/app.43481

INTRODUCTION

Polyurethane (PU) is one of the most important classes of polymers with distinctive structural features and technical applications.[1] Polyurethanes have been frequently employed in engineering components, electrical encapsulation, mineral extraction industry, foams, medical implants, paints, coatings, sealants, and adhesive.[2] These polymers exhibit varying characteristics ranging from rigid thermoplastic to thermoset materials. Various synthetic strategies have been developed to control the polymer properties for diverse potential applications.[3] Important factors in this regard are (i) molecular weight of reactants i.e. polyols and diisocyante; (ii) nature of chain extender; (iii) functionality control; and (iv) chemical composition of PU backbone. For example, poly(ethylene glycol) (PEG) as soft segment has been known to influence the morphology and tensile properties of polyurethane.[4] Moreover, carbon nanofillers have been introduced to increase the mechanical, thermal, and electrical properties of PU-based nanocomposite for technical applications.[5] Polyurethanes also exhibit interesting shape-memory properties. The polymers are set in a particular shape above glass transition temperature (T_g) and cooled to a temperature below T_g. The cooled material holds this particular shape at temperature below T_g. When PU is heated to a temperature above T_g, the polyurethane return to their original shape. The shape-memorizing property of PU may be ascribed to molecular motion of soft segments.[6] The hard segments form physical cross links due to hydrogen bonding, polar interaction, and crystallization in hard domain. This shape-memory effect is usually induced by thermal stimulation, electric field, chemicals, and pH.[7–9]

Polymer blending is also a technique used for the improvement of polymer properties. In this regard polyacrylate blends with functional characteristics have been reported.[10,11] The copolymers of polyacrylate usually contain high-molecular weight ethylene and acrylate monomeric units in the backbone. The acrylate units offer thermal stability while ethylene units provide strength to the copolymer.[12] Incidentally, poly(ethylene-*co*-ethyl acrylate) is an important polymer for blending.[13] Introduction of large pendant groups may decrease the backbone interaction and strength of polyacrylates.[14] However, functional polyacrylate show fine miscibility with polyacetates or other polymers compared with the nonfunctional one. Carbon black (CB) is one of the most commonly employed carbon nanofiller having superior features such as high electrical conductivity, chemical stability, and low cost.[15] CB is known to form conductive network within the polymer matrix to improve the electrical and thermal

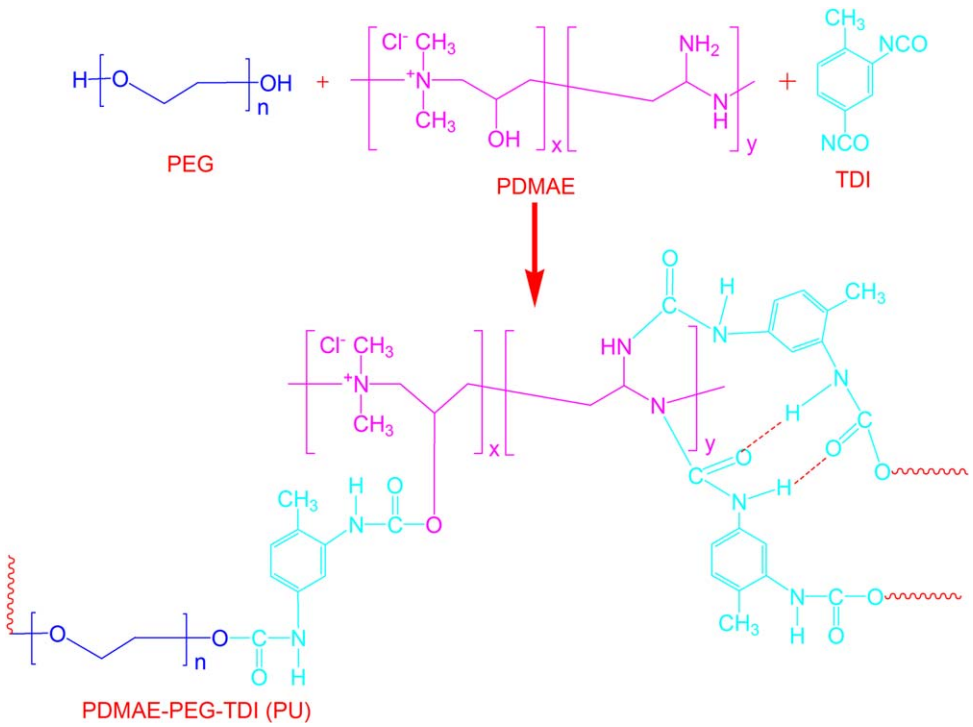

Figure 1. Preparation of polyurethane (PDMAE-PEG-TDI). [Color figure can be viewed in the online issue, which is available at wileyonlinelibrary.com.]

characteristics of CB filler composites.[16] However, higher CB loading may negatively affect the mechanical properties of composite.[17] The growth of fine conductive network within the matrix and reduction in percolation threshold are challenging.[18,19] Mechanical mixing of CB with polyacrylates often produce phase segregated structure. One of the most frequent ways for the reduction of percolation threshold and improvement in physical properties at low CB content is to utilize two-component polymer blends.[20] The properties of such hybrids depend on (i) interface between two phases and CB; (ii) CB dispersion; and (iii) CB content.[21] By controlling these factors the percolation threshold may be significantly reduced.[22] In this attempt we have prepared a polyurethane with poly(dimethylamine-*co*-epichlorohydrin-*co*-ethylenediamine) (PDMAE) and polyethylene glycol (PEG) acting as soft segment and 2,4-toluene diisocyanate (TDI) behaving as hard segment. Later blend of polyurethane (PU) and poly(ethylene-*co*-ethyl acrylate) (PEEA) was developed. In literature the cross-linked polyurethane/acrylic hybrids have been reported.[23] The mechanical properties of polyurethane/acrylic hybrids were found to improve compared with the neat blend components. The improved properties of physical blends were attributed to increase in inter-phase compatibility and improved phase dispersion.[24,25] In this study, PU/PEEA blend was reinforced with functional CB (0.1–1 wt %). Functionalization of CB was employed to induce better interaction and compatibility between the blend components and nanofiller. Afterwards the morphological, mechanical, and shape memory studies have been performed to explore the composite structure. In this study, the shape recovery of PU/PEEA/CB-PVA hybrid was investigated using two strategies (i) by applying thermal heating and (ii) by applying different voltage. This achievement may lead to the application of shape-memory polymers as electroactive actuators which is important in several practical applications such as smart actuators for monitoring microaerial vehicles.

EXPERIMENTAL

Chemicals

Poly(ethylene-*co*-ethyl acrylate) (PEEA, ethyl acrylate 18 wt %, beads, melt index 20 g/10 min), poly(dimethylamine-*co*-epichlorohydrin-*co*-ethylenediamine) (PDMAE, average M_w ~75,000), polyethylene glycol (PEG, M_w ~11,000–13,700), poly(vinyl alcohol) (PVA, M_w 13,000–23,000), 2,4-toluene

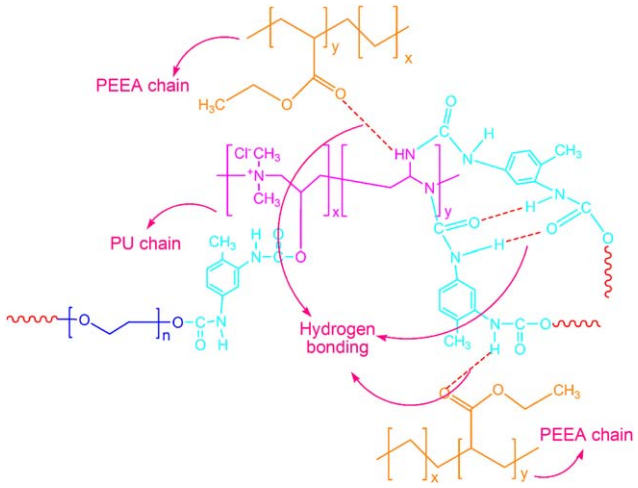

Figure 2. PU/PEEA blend formation. [Color figure can be viewed in the online issue, which is available at wileyonlinelibrary.com.]

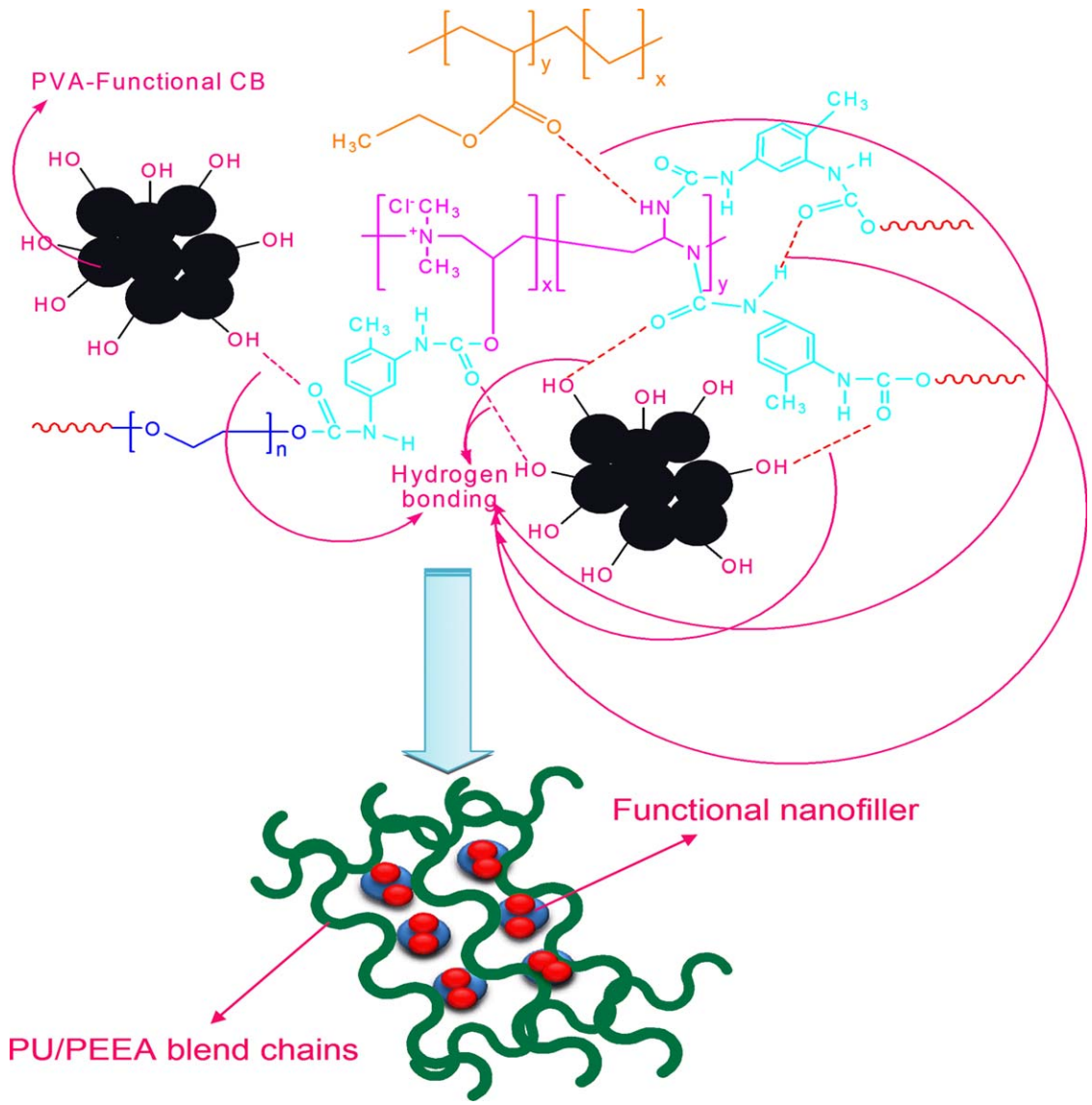

Figure 3. Interaction in PU/PEEA and PVA-functional CB nanoparticle. [Color figure can be viewed in the online issue, which is available at wileyonlinelibrary.com.]

diisocyanate (TDI, 99%) and tetrahydrofuran (THF, 99.5%) were procured from Aldrich. Carbon black (CB, nanopowder <100 nm particle size) was also obtained from Aldrich.

Instrumentation

Infrared (IR) spectra were recorded using Excalibur Series FT-IR Spectrometer, FTSW 300 MX manufactured by BIO-RAD, in transmission mode (4000–400 cm^{-1}). Field Emission Scanning Electron Microscopy (FE-SEM) of fractured samples was performed using Scanning Electron Microscope S-4700 (Japan Hitachi Co. Ltd.). Transmission electron microscopy (TEM) was performed with a JEOL JEM 2100F TEM. The samples were prepared using a Leica UC-6 ultra-microtome with a Diatome diamond knife at room temperature. The samples were fractured under liquid nitrogen, and then vacuum-coated with thin gold layer before analysis. The stress-strain behavior of the samples ($50 \times 10 \times 1 \pm 0.03$ mm^3) was examined using universal testing machine (Instron 4466) and ASTM D638 standard method. The crosshead speed of 20 mm/min was used during the test. Differential scanning calorimetry (DSC) was performed using Perkin-Elmer DSC (Boston, MA). Five milligrams of samples were analyzed at heating rate of 10 °C/min and nitrogen flow rate of 20 mL/min. X-ray diffraction patterns were obtained at room temperature using X-ray diffractometer (3040/60 Xpert PRO) with Ni-filtered Cu Kα radiation (40 kV, 30 mA). The electrical conductivity of thin films was measured at room temperature using the four-point method (Keithley 2401). The samples of rectangular geometry with dimensions of $20 \times 10 \times 1 \pm 0.03$ mm^3 were used for conductivity measurement. The shape-memory effect of rectangular strips with dimension $35 \times 10 \times 1 \pm 0.05$ mm^3 was observed by heating the samples at 60 °C, while monitoring the shape recovery by using a video camera. The shape recovery was calculated using following eq. (1).

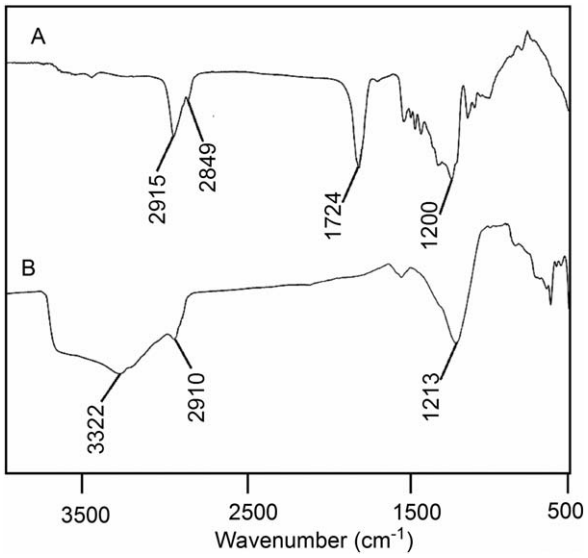

Figure 4. FT-IR spectra of (A) neat PEEA and (B) CB-PVA.

$$SR(\%)=\{(90-\theta)/90\}\times 100 \quad (1)$$

where θ in degree symbolizes the angle between the tangential line at the midpoint of the sample and the line joining the midpoint and the end of the curved samples. Strain fixation rate R_f was measured using eq. (2).

$$R_f = \varepsilon_1/\varepsilon_2 \quad (2)$$

where ε_1 is bending in tension-free state after cooling below T_m; and ε_2 is expansion. The electrical conductivity of thin blend and hybrid films was measured at room temperature and ambient atmosphere using the four-point method (Keithley 2401). The samples of rectangular geometry with dimensions of 35 × 10 × 1 ± 0.05 mm^3 were used for conductivity measurements. The shape-memory effect of rectangular strips with dimension was also observed at 25 and 40 V.

Functionalization of Carbon Black (CB-PVA)

One gram of CB was refluxed in 50 mL HNO_3 (1M aqueous solution) for 4 h. The product was isolated through centrifugation and washed several times with deionized water to attain neutral pH. Finally black powder was vacuum-dried at 80 °C.[26] Afterwards the acid treated CB was functionalized with PVA. In a typical reaction, 1 g acid treated CB was suspended in 10 mL DMSO with ultrasonication of 2 h (30 °C). A solution of PVA in DMSO (1 mg/mL, 10 mL) was added to the suspension and the mixture was sonicated for another 2 h at 30 °C. The product was filtered and dried at 60 °C for 4 h. FT-IR (KBr, cm^{-1}): 3400 (0–H stretch), 2901, 2889 (aliphatic C—H stretch), 1301 (C—O stretch).

Synthesis of PDMAE-PEG-TDI Polyurethane (PU)

The polyurethane, PDMAE-PEG-TDI, was synthesized by addition polymerization. PDMAE and PEG were used as soft segments while TDI was employed as hard segment. The molar ratio of NCO/OH was taken as 1.06 indicating 51 wt % of hard segment content. The desired amount of PDMAE and PEG (0.1:0.9) and THF were charged into a three-necked round bottom flask equipped with a thermometer, reflux condenser, and heating bath. The mixture was stirred for 3 h at 60 °C.[27] Afterwards the preferred amount of TDI was added drop wise with constant stirring. The polyurethane solution prepared was cast into glass Petri dish at room temperature. The dried PU film was obtained with thickness of 1 ± 0.02 mm. The chemical route for the synthesis of PU is shown in Figure 1. FT-IR (Film, cm^{-1}): 3420 (N—H stretch), 3029 (aromatic C—H stretch), 2955 (aliphatic C—H stretch), 1732 (urethane C═O stretch), 1690 (urea C═O stretch), 1596 (N—H bend), 1270 (C—O stretch).

Synthesis of PU/PEEA Blend

For blend preparation, 1.5 g of above prepared polyurethane was refluxed in 10 mL THF at 60 °C for 2 h. PEEA (0.5 g) was dissolved in 5 mL THF and added to the PU solution. The mixture was refluxed at 60 °C for 6 h. The mixture was poured in glass Petri dish to obtain PU/PEEA blend film (Figure 2). The dried film had thickness of 1 ± 0.01 mm. FT-IR (Film, cm^{-1}): 3311 (N—H stretch), 3011 (aromatic C—H stretch), 2931 (aliphatic C—H stretch), 1727 (urethane C═O stretch), 1715 (ester C═O stretch), 1670 (urea C═O stretch), 1588 (N—H bend), 1244 (C—O stretch).

Synthesis of PU/PEEA/CB-PVA Hybrid

In a typical procedure, solution of 1.5 g PU was refluxed in 10 mL THF at 60 °C for 2 h. PEEA (0.5 g) was dissolved in 5 mL THF separately. Both solutions were mixed and refluxed at 60 °C (6 h) to obtain blend mixture. Afterwards the desired weight fraction of CB-PVA (0.1, 0.3, 0.5, and 1) was dispersed in 10 mL THF with 3 h sonication. The dispersed filler mixture was then added to the blend mixture and refluxed at 60 °C for 4 h. Finally, hybrid film was obtained by solution casting at room temperature. The dried films were obtained with thickness of 1 ± 0.03 mm. Schematic illustration of PU/PEEA/CB hybrid

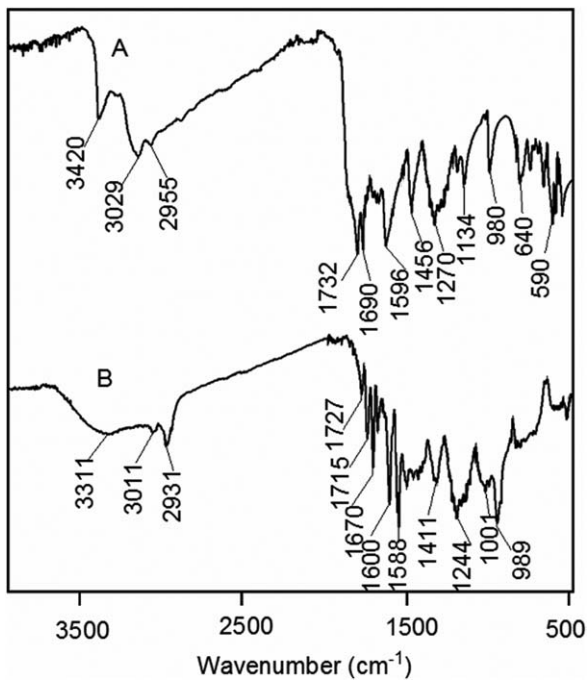

Figure 5. FT-IR spectra of (A) PU; (B) PU/PEEA blend.

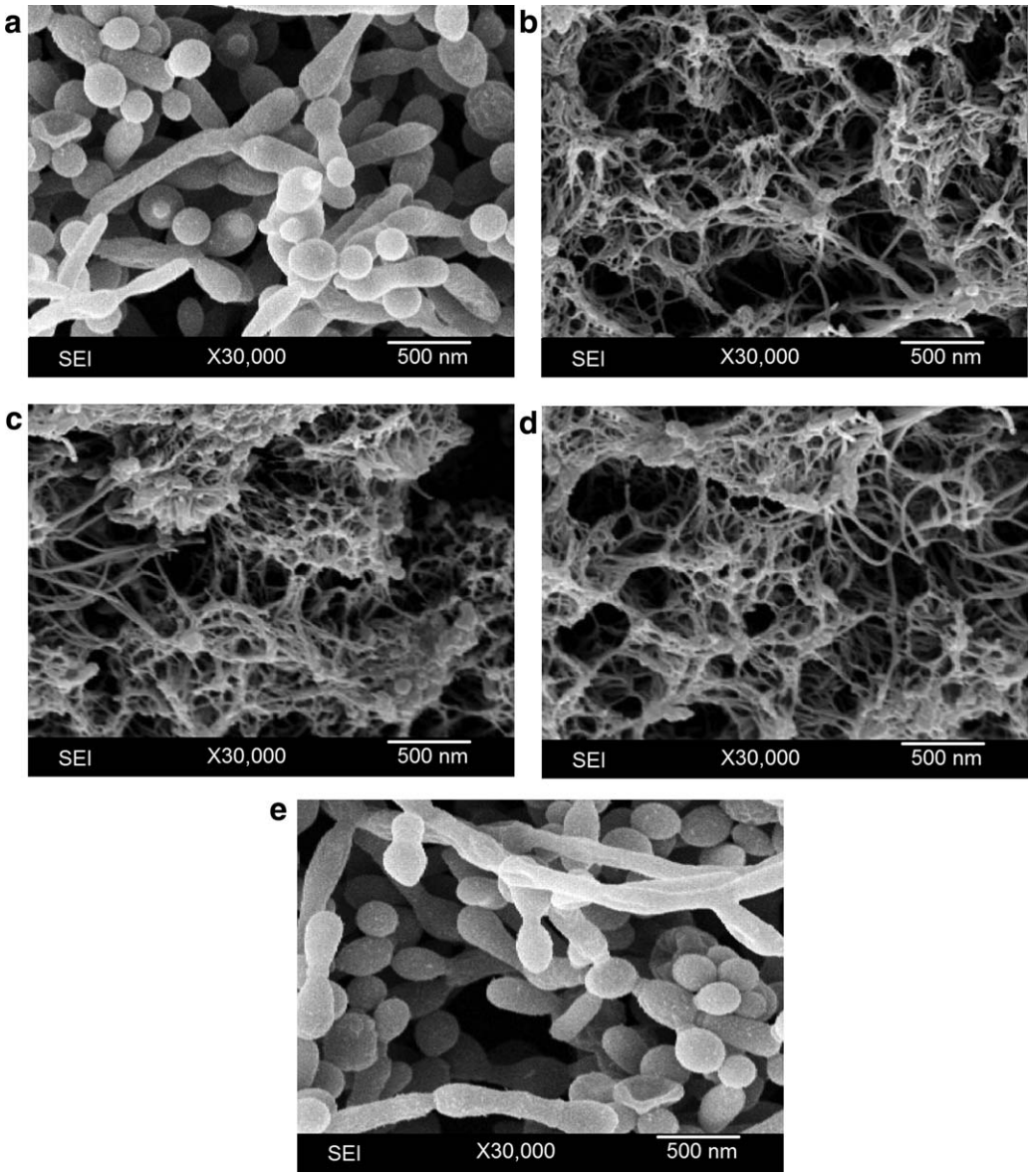

Figure 6. FESEM micrographs (A) PU/PEEA blend; (B) PU/PEEA/CB-PVA 0.1; (C) PU/PEEA/CB-PVA 0.3; (D) PU/PEEA/CB-PVA 0.5; and (E) PU/PEEA/CB-PVA 1 hybrid.

is shown in Figure 3. FT-IR (Film, cm^{-1}): 3299 (N—H stretch), 3008 (aromatic C—H stretch), 2901 (aliphatic C—H stretch), 1721 (urethane C=O stretch), 1711 (ester C[dond]O stretch), 1667 (urea C=O stretch), 1580 (N—H bend), 1240 (C—O stretch).

RESULTS AND DISCUSSION

FT-IR Analysis of Polyurethane and Hybrid

A survey of IR spectra of polyurethane and PEEA and PVA-CB (400–4000 cm^{-1}) at room temperature is shown in Figure 4A and B. Neat PEEA depicted aliphatic C—H stretching vibration at 2849 and 2915 cm^{-1} [Figure 4(A)]. The ester C=O stretching band appeared at 1724 cm^{-1}. The broad C—O stretching vibration was also observed in the spectrum at 1200 cm^{-1}. In CB-PVA spectrum, the broad band at 3300 to 3500 cm^{-1} was identified with O–H stretching vibrations due to hydroxyl groups of PVA [Figure 4(B)]. The presence of C—O group was confirmed at 1213 cm^{-1}. Moreover aliphatic C—H stretching vibration appeared at 2910 cm^{-1}. In polyurethane, a strong band at 3420 cm^{-1} was assigned to N—H stretching vibration [Figure 5(A)]. The N—H bending vibration of urethane group was also found at 1596 cm^{-1}. The aliphatic asymmetric C—H stretching vibration was observed at 2955 cm^{-1}, while aromatic C—H stretch appeared at 3029 cm^{-1}. The formation of PDMAE-PEG-TDI was also confirmed by the presence of urea and urethane carbonyl linkages. The band at 1732 cm^{-1} was assigned to the urethane C=O stretch, while that at 1690 cm^{-1} was assigned to the urea C=O stretch. The broad band at 1270 cm^{-1} was assigned to C—O stretch. The observed peaks in the spectrum indicated the formation of polyurethane. In PU/

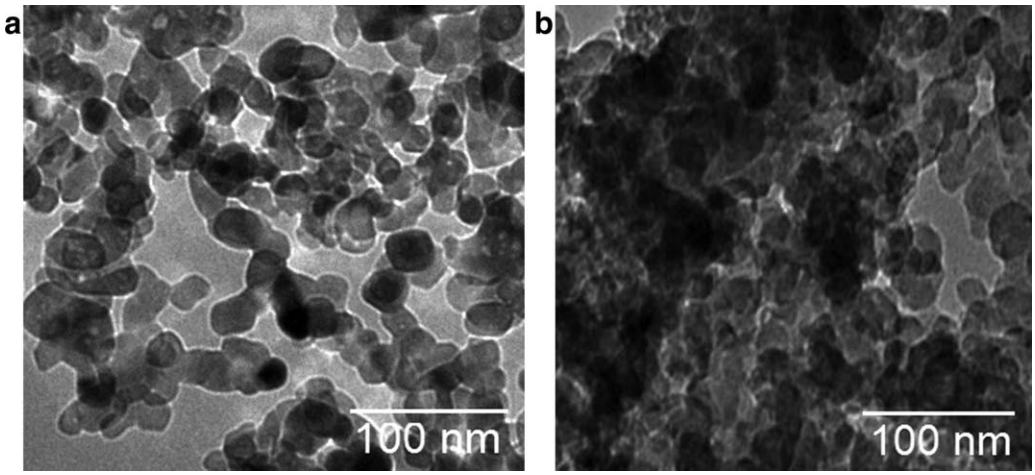

Figure 7. TEM images of (A) CB and (B) CB-PVA.

PEEA blend, the hydrogen bonded N—H band absorbance was decreased [Figure 5(B)]. The bonded N—H band was shifted from 3420 cm^{-1} to 3311 cm^{-1}. According to literature, the band detected at 3311 cm^{-1} may also be attributed to the combination of the stretching modes of OH functionalities of the acrylic, water, and hydrogen bonded N—H group.[28] There was also a shift in the absorption band of N—H bending vibration. The N—H be of urethane group therefore appeared at 1588 cm^{-1}. Similar to the PU spectrum, aliphatic and aromatic C—H stretching vibration appeared at 2931 and 3011 cm^{-1}. It was noted that in PU/PEEA the carbonyl band absorbance was dependent on the interaction between the blend components (C═O……..N—H). There exist different types of hydrogen bonding interaction in blend and nanocomposite. Figures 2 and 3 show only some hydrogen bonding interaction existing between PU and PEEA chains. Some weaker hydrogen bonds between urethane groups are also mentioned. Consequently the lowering in urethane and urea carbonyl towards 1727 and 1670 cm^{-1} depicted hydrogen bonding between PEEA and rigid PU segments. Absorbance of bonded ester C═O stretching band appeared at 1715 cm^{-1}. The absorbing intensity of the strong carbonyl peak was also found in literature for core-shell polyurethane cross-linked polyacrylates.[29,30] The broad C—O stretching vibration was also observed in the spectrum (1244 cm^{-1}). Further lowering of peaks in PU/PEEA/CB-PVA 1 hybrid was observed due to increased interaction between blend components and PVA functional CB nanoparticles. The structure and physical interaction in compatible blends and nanocomposite were well confirmed from the spectrum.

Morphology Study

Scanning electron micrographs of PU/PEEA blend is given in Figure 6(A). Due to noncovalent interaction of blend components, higher compatibility was expected. However the micrographs showed some interlinked globular domains in which two polymers could not be identified. The morphology of PU/PEEA/CB-PVA hybrids was entirely different than the neat blend. In PU/PEEA/CB-PVA 0.1, both the polyurethane and poly(ethylene-*co*-ethyl acrylate) formed a continuous phase [Figure 6(B)]. The physically inter-linked polymers were well-dispersed and locally interconnected. Interaction between blend component and nanoparticles initiated self-assembled structure.

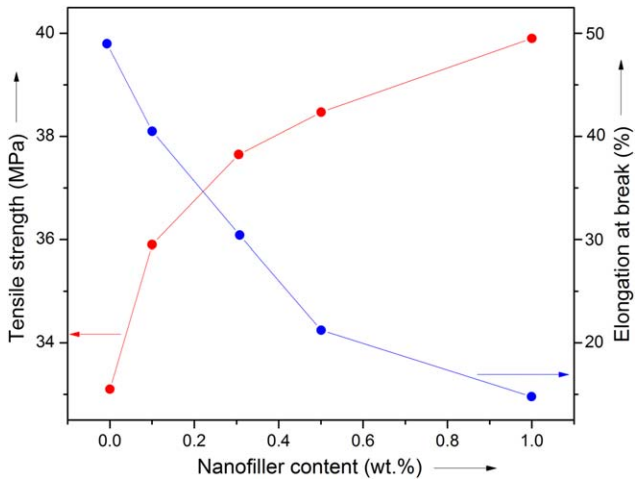

Figure 8. Mechanical properties of PU/PEEA blend and PU/PEEA/CB-PVA hybrids. [Color figure can be viewed in the online issue, which is available at wileyonlinelibrary.com.]

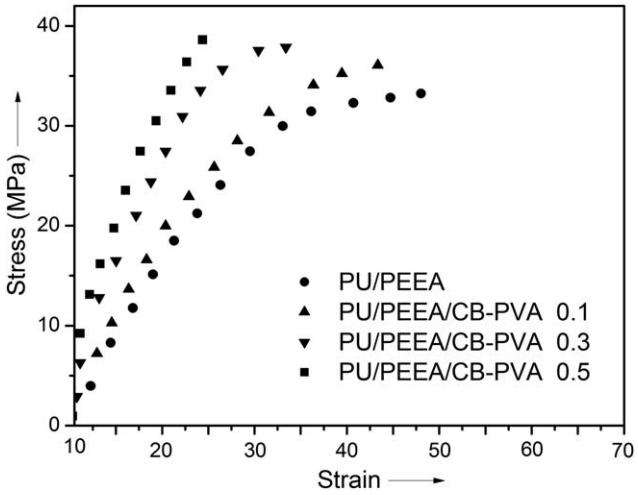

Figure 9. Stress–strain curves of PU/PEEA/CB-PVA hybrids.

Table I. Mechanical properties of polyurethane, blend, and PU/PEEA/CB-PVA hybrids

Sample	Tensile strength (MPa)	Strain (%)	Young's modulus (GPa)
PU	26.7	50.1	13.2
PU/PEEA	33.1	49.2	18.5
PU/PEEA/CB-PVA 0.1	35.9	43.2	23.4
PU/PEEA/CB-PVA 0.3	37.6	32.5	33.8
PU/PEEA/CB-PVA 0.5	38.5	22.3	38.8
PU/PEEA/CB-PVA 1	39.9	10.1	40.4

Functional CB directed self-assembled network structure i.e. often named as interpenetrating network (IPN) in the resulting hybrid materials. With the increase in nanofiller content, the polyurethane-poly(ethylene-*co*-ethyl acrylate) copolymer phase retained continuity [Figure 6(C)]. The self-assembled IPN structure attain finer outline with the functional nanofiller loading.[31,32] The reason might be the increased interaction between the blend and nanofiller at higher loading level [Figure 6(D)]. However the IPN morphology with 1 wt % functional nanofiller became complicated since both phases assume globular morphology. The morphology investigation suggest that the physically linked copolymer network was formed at 0.1 to 0.5 wt % loading, while at further higher loading the IPN was distorted. TEM micrographs of CB and CB-PVA functional nanoparticle are shown in Figure 7. The micrographs have shown carbon black particles smaller than 100 nm [Figure 7(A)]. The PVA functionalized nanoparticles were also smaller than 100 nm while some agglomerates were found larger than 100 nm [Figure 7(B)]. The structure of the particles appears to be unique and easy to identify. Polymer formulations containing carbon black particles depicted unique morphology as discussed earlier.

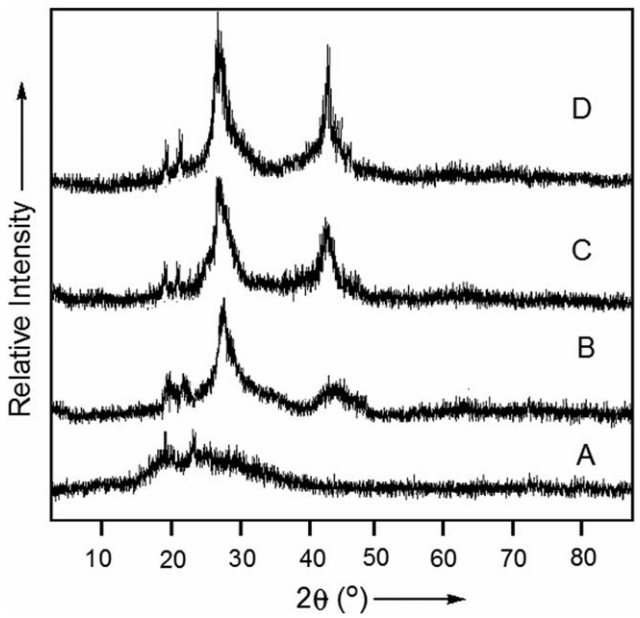

Figure 10. X-ray diffraction patterns of (A) PU/PEEA blend; (B) PU/PEEA/CB-PVA 0.1; and (C) PU/PEEA/CB-PVA 0.5; (D) PU/PEEA/CB-PVA 1.

Mechanical Property Study

Figure 8 illustrates the mechanical properties of specimens, which shows increased tendency of tensile strength and reduced trend for elongation at break. The neat polyurethane showed tensile strength of 26.7 MPa, which increased to 33.1 MPa in PU/PEEA blend. In hybrid system with increasing CB-PVA content, the tensile strength increased from 35.9 to 39.9 MPa (Figure 9). The elongation at break was decreased from 49.2 to 10.1%. Generally higher the content of nanoparticle in the polymer matrix, the more brittle is the nanocomposites. For the presence of higher functional CB content, molecular chain motion was resisted. Mechanical properties of novel hybrids are reported in Table I. The Young's modulus for PU/PEEA/CB-PVA 0.1-1 hybrids was also increased from 23.4 to 40.4 GPa with filler addition. Consequently, Young's modulus for PU/PEEA (18.5 GPa) was 71% higher than neat polyurethane (13.2 GPa). Generally polymer/carbon black nanocomposite show tremendous improvement in mechanical properties including modulus and strength. Young's modulus of carbon black-based nanocomposite may be ~50% greater than the baseline matrix.[33,34] In PU/PEEA-based nanocomposite, addition of carbon black filler has shown tremendous potential for mechanical-property enhancement due to the combination of high specific surface area, strong nanofiller-matrix adhesion and the outstanding mechanical properties of functional carbon bonding network. These results suggested that the functional CB nanoparticle had greater influence on the mechanical properties of PU/PEEA blends.[35]

Crystallization Property Investigation

The crystallization property of blend and hybrids was determined by XRD and DSC tests. The typical XRD patterns of blend, PU/PEEA/CB-PVA 0.1, PU/PEEA/CB-PVA 0.5, and PU/PEEA/CB-PVA 1 are given in Figure 10. In the blend structure two well-defined peaks appeared at $2\theta = 20.1°$ and $2\theta = 22.4°$. These diffraction peaks were attributed to the polymer fraction of PEG. The peaks appeared due to the ordered arrangement of

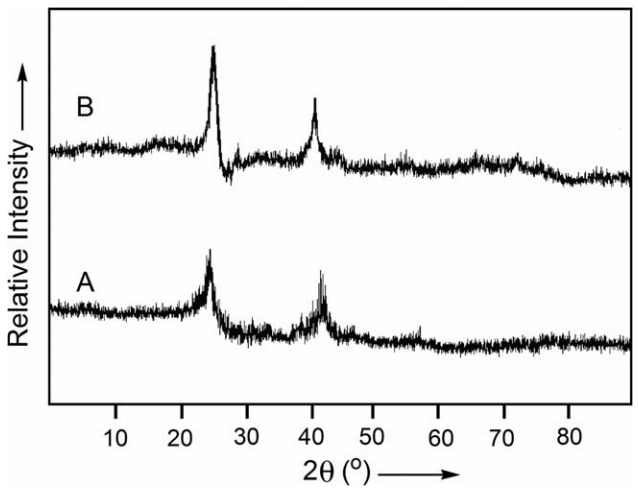

Figure 11. X-ray diffraction patterns of (A) CB and (B) CB-PVA.

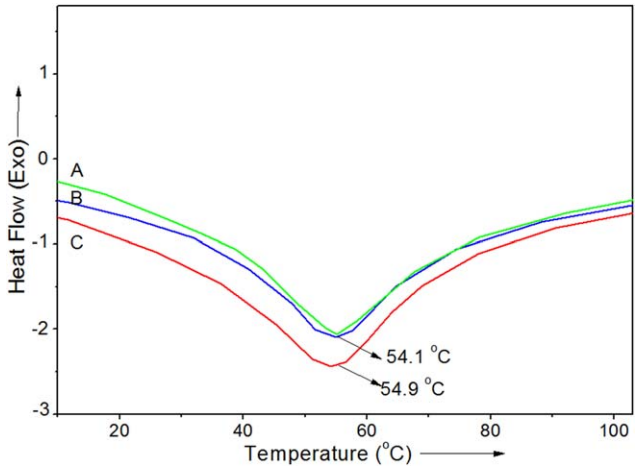

Figure 12. DSC second covers of samples: (A) PU/PEEA/CB-PVA 0.1; (B) PU/PEEA/CB-PVA 0.5; and (C) PU/PEEA/CB-PVA 1. [Color figure can be viewed in the online issue, which is available at wileyonlinelibrary.com.]

polyurethane soft segments and non-covalent interaction between the blend components. As a result polymer chains were inclined to crystallize generating some crystalline peaks. The result suggests that the sample was partially crystallized (semi-crystalline) in nature [Figure 10(A)]. From Figure 10(B,C), in addition to blend peaks two more diffraction peaks can be seen clearly. Diffraction peaks of PU/PEEA did not shift in the hybrid spectra. It may be concluded that the embedded carbon black nanoparticles do not result in a change of crystal structure of the blend matrix. However functional carbon black peaks appeared at $2\theta = 23.2°$ (002) and $2\theta = 42.2°$ (100). The position of the peak corresponding to the $2\theta = 22.9$ (002) and $2\theta = 41.9°$ (100) graphitic planes (d-spacing of 0.37 nm) of virgin CB-PVA was compared with functional CB-PVA, as shown in Figure 11. No significant difference in either the position of the peak or the area under the curve was observed indicating no observable changes in the graphitic content of the carbon black as a result

Table II. Heat induced shape recovery effect in blend and hybrids

Sample	Shape recovery rate (%)	Recovery time (s)	Shape recovery (%)	R_f (%)
PU	38	20.8	82	37
PU/PEEA	40	13.11	92	39
PU/PEEA/CB-PVA 0.1	64	12.09	93	64
PU/PEEA/CB-PVA 0.3	65	9.97	93	65
PU/PEEA/CB-PVA 0.5	70	8.88	94	71
PU/PEEA/CB-PVA 1	76	7.98	94	76

of functionalization. The intensity of CB peaks however was increased with the nanofiller loading in the hybrid structure.[36] This was further confirmed by DSC analysis. Figure 12 shows DSC second thermograms curves of blend, PU/PEEA/CB-PVA 0.1, PU/PEEA/CB-PVA 0.5, and PU/PEEA/CB-PVA 1. The melting temperature (T_m) was studied using DSC analysis. The melting peak appeared due to the presence of polyethylene glycol soft segment. According to the thermograms, T_m only slightly increased with the incorporation of CB nanoparticles due to the heat absorption process. This result means that the CB loading did not significantly affect the melting temperature of blend phase.[37] The melting enthalpy (ΔH_m) of the hybrids was ~70 J/g.

Heat-Induced Shape Memory versus Electroactive Shape Memory

Heat induced shape memory properties of PU/PEEA/CB-PVA hybrids are shown in Table II. The blend exhibited shape memory property upon the addition of CB. The shape memory behavior was observed by first bending the samples in U-shaped at transition temperature (T_{trans}), followed quenching to room temperature to obtain temporary shape and finally reheating it. The value of T_{trans} was taken 60 °C, closer to the T_m obtained from DSC studies.[38,39] When a surface temperature of 60 °C was

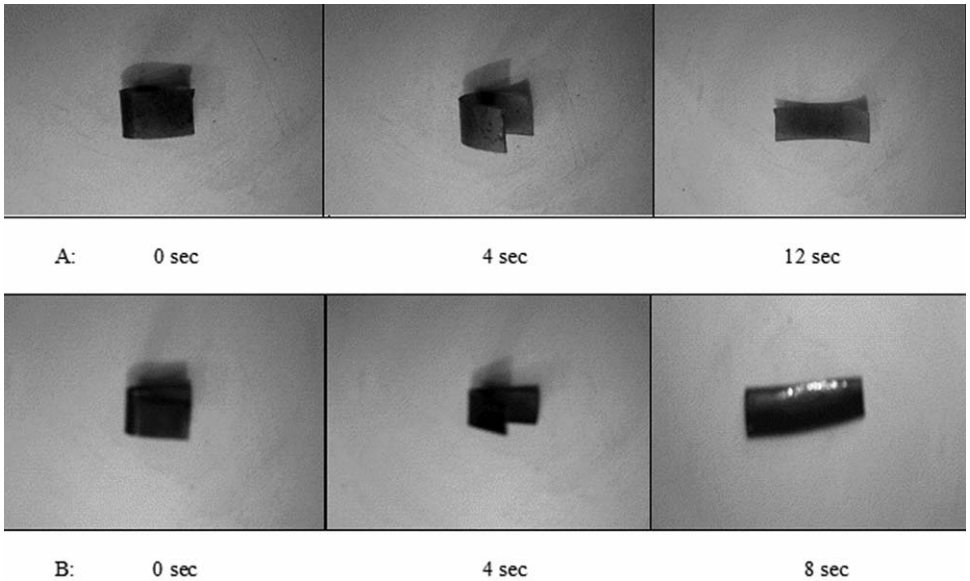

Figure 13. The process of thermo-responsive shape memory recovery of (A) PU/PEEA/CB-PVA 0.1 and (B) PU/PEEA/CB-PVA 1 at 60 °C.

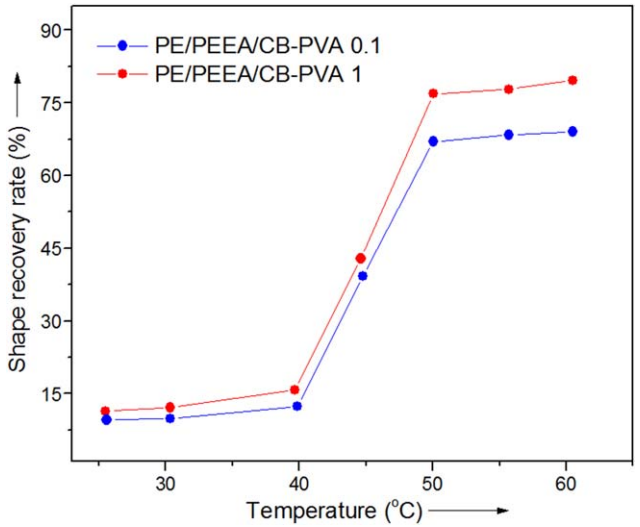

Figure 14. Thermo-responsive shape recovery rate of hybrids at different temperature. [Color figure can be viewed in the online issue, which is available at wileyonlinelibrary.com.]

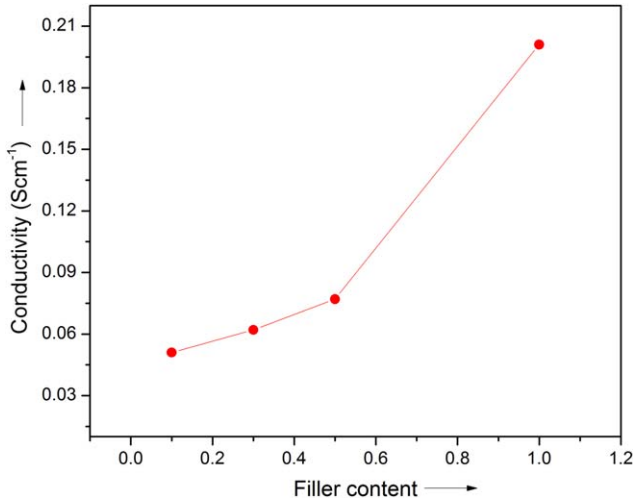

Figure 15. Conductivity of PU/PEEA/CB-PVA hybrids. [Color figure can be viewed in the online issue, which is available at wileyonlinelibrary.com.]

given to the samples, shape was changed spontaneously into that shown in Figure 13. The original shape of the samples was nearly 92 to 94% recovered approximately within 60 s. At a temperature below T_m 25 to 40 °C, shape recovery rate was lower (Figure 14). The shape memory hybrid gained high shape recovery rate at 45 to 50 °C. When the temperature was higher than 50 °C, the shape recovery rate reached maximum value. The strain fixity is also mentioned in Table II. The electrical conductivity of PU/PEEA blend was found to be increased with increase in weight % of the conductive component i.e., CB. Curves are displayed in Figure 15 and the results are listed in Table III. Notably, the incorporation of conductive CB into the PU/PEEA resulted higher values of conductivity compared to blend. The hybrids revealed conductivity in the range of 0.051 to 0.201 Scm^{-1} while neat polyurethane (0.72×10^{-8} Scm^{-1}) and blend (0.79×10^{-8} Scm^{-1}) possess lower conductivity. Therefore the response of PU and PU/PEEA towards electric field induced shape recovery was very low. Electric field-triggered shape recovery of the blend and hybrids is also shown in Table III. The rectangular strip of PU/PEEA/CB-PVA 1 sample was deformed into a round shape by using liquid nitrogen. When constant voltage (40 V) was applied, its shape changed impulsively. The original shape of the sample was almost 97% recovered in 6s (PU/PEEA/CB-PVA). The hybrids showed better shape recovery of 94 to 97% within 6 to 10 s (Figure 16). Moreover, the good electrical conductivity at higher filler loading and optimal mechanical properties was important to demonstrate the electroactive shape memory behavior in hybrids relative to simple heating alone.

Table III. Electrical conductivity and electroactive shape recovery of blend and hybrids

Composition	Electrical conductivity (Scm^{-1})	Shape recovery (%)	Recovery time (s)
PU	0.72×10^{-8}	20	30.8
PU/PEEA	0.79×10^{-8}	23	31.9
PU/PEEA/CB-PVA 0.1	0.051	94	8.09
PU/PEEA/CB-PVA 0.3	0.062	95	7.97
PU/PEEA/CB-PVA 0.5	0.077	96	6.66
PU/PEEA/CB-PVA 1	0.201	97	5.99

CONCLUSIONS

Shape memory hybrids of PU/PEEA/CB-PVA were fabricated using solution technique. The physically interlinked blend of polyurethane and poly(ethylene-*co*-ethyl acrylate) was prepared and reinforced with PVA functional carbon black nanoparticles. The formation of interpenetrating network was revealed by SEM analysis. The IPN was intern responsible for mechanically

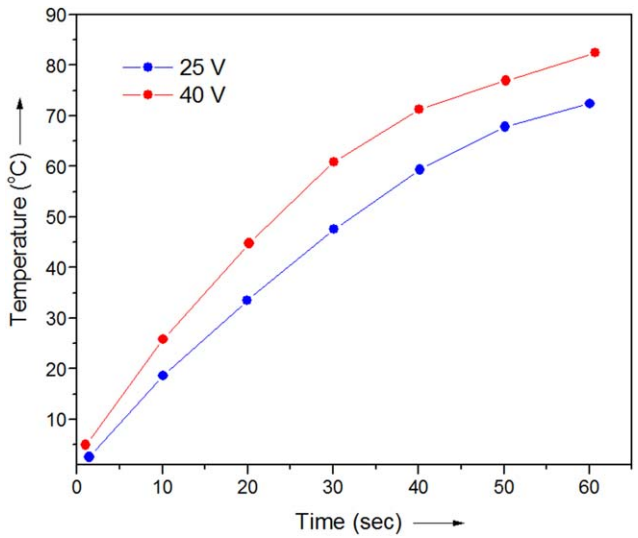

Figure 16. Temperature change of PU/PEEA/CB-PVA 1 with time at different voltage. [Color figure can be viewed in the online issue, which is available at wileyonlinelibrary.com.]

robust hybrid system. The results showed that Young's Modulus and tensile strength of hybrids were increased significantly relative to pure PU and PU/PEEA blend even with lower filler content (0.1–1 wt %). The electrical conductivity of PU/PEEA/CB-PVA 1 hybrid was increased up to 0.201 Scm^{-1}. The electrical conductivity was sufficient for the hybrid to reveal electroactive shape memory with bending mode. The original shape of the sample was almost 97% recovered in an electric field of 40 V.

REFERENCES

1. Manvi, G. N.; Singh, A. R.; Jagtap, R. N.; Kothari, D. C. *Prog. Org. Coat* **2012**, *75*, 139.
2. Gartia, Y.; Moore, J.; Felton, C.; Pulla, S.; Berry, B.; Munshi, P.; Ghosh, A. *J. Appl. Polym. Sci.* **2013**, *128*, 3522.
3. Yang, H. Y.; Zhang, X. M.; Duan, L. J.; Zhang, M. Y.; Gao, G. H.; Zhang, H. X. *J. Appl. Polym. Sci.* **2013**, *129*, 846.
4. Mao, H.; Qiang, S.; Yang, F.; Zhao, C.; Wang, C.; Yin, Y. *J. Appl. Polym. Sci.* **2015**, *132*. DOI: 10.1002/app.42780.
5. Leng, J.; Lan, X.; Liu, Y.; Du, S. *Prog. Mater. Sci* **2011**, *56*, 1077.
6. Gunes, I. S.; Cao, F.; Jana, S. C. *Polymer* **2008**, *49*, 2223.
7. Takahashi, T.; Hayashi, N.; Hayashi, S. *J. Appl. Polym. Sci* **1996**, *60*, 1061.
8. Zhang, L.; Brostowitz, N. R.; Cavicchi, K. A.; Weiss, R. A. *Macromol. React. Eng.* **2014**, *8*, 81.
9. Jaudouin, O.; Robin, J. J.; Lopez-Cuesta, J. M.; Perrin, D.; Imbert, C. *Polym. Int.* **2012**, *61*, 495.
10. Guo, Y. H.; Li, S. C.; Wang, G. S.; Ma, W.; Huang, Z. *Prog. Org. Coat.* **2012**, *74*, 248.
11. Shah, R.; Kausar, A.; Muhammad, B. *Polym. Plast. Technol. Eng.* **2015**, *54*, 1334.
12. Morgan, A. B.; Cogen, J. M.; Opperman, R. S.; Harris, J. D. *Fire. Mater.* **2007**, *31*, 387.
13. Lee, K. Y.; Kim, K. Y.; Han, W. Y.; Park, D. H. *Dielect. Elect. Insulat. IEEE. Trans.* **2008**, *15*, 205.
14. Nuhn, L.; Overhoff, I.; Sperner, M.; Kaltenberg, K.; Zentel, R. *Polym. Chem.* **2014**, *5*, 2484.
15. Sun, L.; Huang, W. M.; Ding, Z.; Zhao, Y.; Wang, C. C.; Purnawali, H.; Tang, C. *Mater. Design* **2012**, *33*, 577.
16. Small, W. I. V.; Singhal, P.; Wilson, T. S.; Maitland, D. J. *J. Mater. Chem.* **2010**, *20*, 3356.
17. Novák, I.; Krupa, I.; Chodák, I. *J. Mater. Sci. Lett.* **2002**, *21*, 1039.
18. Xu, Z.; Zhao, C.; Gu, A.; Fang, Z.; Tong, L. *J. Appl. Polym. Sci.* **2007**, *106*, 2008.
19. Yang, Q. Q.; Liang, J. Z. *J. Appl. Polym. Sci.* **2010**, *117*, 1998.
20. Zhao, X.; Zhao, J.; Cao, J. P.; Wang, X.; Chen, M.; Dang, Z. M. *J. Phys. Chem. B* **2013**, *117*, 2505.
21. Xu, X. B.; Li, Z. M.; Yu, R. Z.; Lu, A.; Yang, M. B.; Huang, R. *Macromol. Mater. Eng.* **2004**, *289*, 568.
22. Gubbels, F.; Blacher, S.; Vanlathem, E.; Jérôme, R.; Deltour, R.; Brouers, F.; Teyssie, P. *Macromolecules* **1995**, *28*, 1559.
23. Madbouly, S. A.; Xia, Y.; Kessler, M. R. *Macromolecules* **2013**, *46*, 4606.
24. You, B.; Zhou, D.; Yang, F.; Ren, X. *Colloid Surf. A* **2011**, *392*, 365.
25. Athawale, V. D.; Kulkarni, M. A. *Pigment. Resin. Technol* **2010**, *39*, 141.
26. Xue, P. F.; Wang, J. B.; Bao, Y. B.; Wu, C. F. *Chin. J. Polym. Sci.* **2012**, *30*, 652.
27. Sattar, R.; Kausar, A.; Siddiq, M. *Chin. J. Polym. Sci.* **2015**, *33*, 1313.
28. Chai, S. L.; Jin, M. M.; Tan, H. M. *Eur. Polym. J.* **2008**, *44*, 3306.,
29. Chai, S. L.; Tan, H. M. *J. Appl. Polym. Sci.* **2008**, *107*, 3499.
30. Dong, A.; Wan, T.; Feng, S.; Sun, D. *J, Polym. Sci. Part B: Polym. Phys.* **1999**, *37*, 2642.
31. Sperling, L. H. In Interpenetrating Polymer Networks and Related Materials; Springer Science & Business Media: New York, **2012**; p 66.
32. Kong, X.; Narine, S. S. *Biomacromolecules* **2008**, *9*, 2221.
33. Borreguero, A. M.; Rodríguez, J. F.; Valverde, J. L.; Peijs, T.; Carmona, M. *J. Appl. Polym. Sci.* **2013**, *128*, 582.
34. Arroyo, M.; Lopez-Manchado, M. A.; Herrero, B. *Polymer* **2003**, *44*, 2447.
35. Praveen, S.; Chattopadhyay, P. K.; Albert, P.; Dalvi, V. G.; Chakraborty, B. C.; Chattopadhyay, S. *Compos. A* **2009**, *40*, 309.
36. Tai, F. C.; Wei, C.; Chang, S. H.; Chen, W. S. *J. Raman Spectrosc.* **2010**, *41*, 933.
37. Yu, X. J.; Zhou, S. B.; Zheng, X. T.; Guo, T.; Xiao, Y.; Song, B. T. *Nanotechnology* **2009**, *20*, 235702.
38. Hu, J.; Yang, Z.; Yeung, L.; Ji, F.; Liu, Y. *Polym. Int.* **2005**, *54*, 854.
39. Yang, Z.; Hu, J.; Liu, Y.; Yeung, L. *Mater. Chem. Phys.* **2006**, *98*, 368.